Creation and direct laser acceleration of positrons in a single stage

Bertrand Martinez[ORCID],[*] Bernardo Barbosa[ORCID], and Marija Vranic[ORCID]

Golp/Instituto de Plasma e Fusão Nuclear, Instituto Superior Técnico,
Universidade de Lisboa, 1049-001 Lisbon, Portugal

Relativistic positron beams are required for fundamental research in nonlinear strong field QED, plasma physics, and laboratory astrophysics. Positrons are difficult to create and manipulate due to their short lifetime, and their energy gain is limited by the accelerator size in conventional facilities. Alternative compact accelerator concepts in plasmas are becoming more and more mature for electrons, but positron generation and acceleration remain an outstanding challenge. Here, we propose a new setup where we can generate, inject, and accelerate them in a single stage during the propagation of an intense laser in a plasma channel. The positrons are created from a laser-electron collision at 90°, where the injection and guiding are made possible by an 800-nC electron beam loading which reverses the sign of the background electrostatic field. We obtain a 17-fC positron beam, with GeV-level central energy within 0.5 mm of plasma.

I. INTRODUCTION

Plasma-based compact particle sources hold great potential for future applications. While conventional accelerators are limited to a maximum acceleration gradient of 10 MV/m due to the material damage threshold, using a plasma allows for sustaining stronger fields (10 GV/m), enabling short acceleration distances. In addition to the high damage threshold, plasmas self-generate fields that are suited to focus electrons [1]. Combining the acceleration and focusing forces, plasmas naturally provide both the acceleration and beam transport for the accelerated electrons. It is, however, arduous to extend this to positrons, as the accelerating structure developed for electrons is usually defocusing for a positron beam and can lead to beam breakup. This makes the acceleration of positrons a particularly challenging problem. Since the first proof of the principle of positron guiding in plasma [2–5], only a limited number of experiments on positron acceleration followed [6–9]. Theoretical works proposed ideas to accelerate positrons by tailoring the driver [10–13] or by tuning the plasma profile [14–21]. This postacceleration of positrons in a plasma enables the creation of high charge and high quality beams. However, it is not a compact solution as it requires creating and transporting a positron beam in a kilometer-long accelerator.

The upcoming 10–200 PW [22–31] laser infrastructures will bring us closer to answering the question "What is the best way to accelerate positrons in a plasma?" The scattering of a relativistic electron beam with a multi-PW laser pulse is predicted to generate gamma rays and electron-positron pairs (through nonlinear Compton scattering and Breit Wheeler pair creation [32]). Numerical studies have explored gamma-ray emission [33–36] or positron creation [37–40] but still miss an in-depth investigation of positron acceleration. To date, very few schemes have been proposed for positron creation and acceleration [41–45] and they all rely on qualitative 2D and/or staged modeling. Consistent modeling of all important steps (creation, injection, and acceleration) in 3D geometry is still missing.

In this work, we propose a new setup to obtain relativistic positron beams using next-generation laser systems (see Fig. 1). Positrons are created and accelerated during the interaction of an intense laser pulse ($\sim 5 \times 10^{23}$ W/cm^2, 80 PW, and 12 kJ of energy) with a relativistic electron beam at 90° of incidence, as first introduced in Ref. [43]. Even though most pairs are generated in the direction of the electron momentum, a fraction can be deflected by the laser field toward its propagation direction. These positrons are then accelerated in vacuum, but their maximum energy is limited by laser defocusing [43]. Here, we derive a semi-analytical model for the number of positrons created and show a few percent is deflected and available for acceleration. We propose to extend the acceleration distance of the pairs using a plasma channel, where the laser can be self-guided and the pairs can experience Direct Laser Acceleration (DLA) [46–54]. We demonstrate that for intense lasers propagating in a plasma channel, a dense central electron beam (~ 800 nC) is self-injected and copropagates with the

---
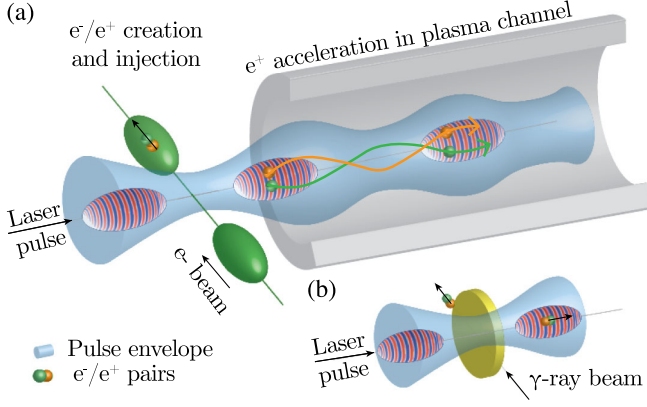[*]bertrand.martinez@tecnico.ulisboa.pt

FIG. 1. (a) Setup: electron-positron pairs (in green/orange) are created during the interaction of an intense laser pulse (blue/red) with a relativistic electron beam (green) at a 90° incidence angle. A fraction of the pairs is injected and propagates with the pulse through the plasma channel, experiencing direct laser acceleration. (b) Quasi-3D modeling of this setup. A slab of γ-ray photons from the electron-laser collision is initialized at $t = 0$.

laser on-axis [55–57]. This beam attracts positrons toward the channel center, enabling their acceleration to GeV energies. We present an analysis of the energy gain induced by different field components and show that a collimated (50 mrad) positron beam of 17 fC can be obtained within 400 μm of laser propagation. This work represents a proof-of-concept that positrons can be created, injected, and accelerated over 0.5 mm of plasma. Higher charge, energy, and positron beam quality are expected by optimizing initial conditions, and it will be a subject of future study.

II. POSITRON GUIDING IN A PLASMA CHANNEL

The setup in Fig. 1 can be modeled using a Particle-In-Cell (PIC) code coupled with a Monte-Carlo module that accounts for pair creation and hard photon emission. A reliable description of laser guiding in a plasma channel requires modeling electromagnetic fields in 3D geometry. However, this is out of reach of modern supercomputers as we estimated it would require 100 million cpu. hours and a total memory of 10 petabytes. Quasi-3D modeling with the OSIRIS [58] framework is possible: an approach where the fields are represented in cylindrical coordinates (z, r, ϕ) using a Fourier decomposition in angular modes [59,60]. The first two modes account for the axisymmetric self-generated channel fields (mode $m = 0$) and for the non-axisymmetric linearly polarized laser field ($m = 1$). With this geometry, we cannot represent the electron beam at 90°, but we can represent the photons it radiates. The assumptions we made and all simulation parameters are in the Supplementary Material [61].

We consider a laser duration of 150 fs, a peak intensity of 5×10^{23} W/cm^2, and a plasma channel with a radial density profile of parabolic shape (density $\sim 10^{19}$–10^{21}/cm^3). As the

laser propagates in the channel, its ponderomotive force repels electrons toward the channel walls, forming a positive radial electric field $\mathbf{E}_c = +|E_c|\mathbf{r}$. This electric field remains positive and persists as long as ion motion is negligible [57]. In addition, the laser electric field extracts electrons in its polarization direction from the channel walls. The magnetic component of the laser can rotate these electrons along the channel axis enabling their injection and making them available for direct laser acceleration. The tenuous electron beam formed drives a negative azimuthal magnetic field $\mathbf{B}_c = -|B_c|\boldsymbol{\phi}$. The resulting transverse Lorentz force $|E_c| + |B_c|$ pulls the copropagating electrons toward the axis. The same force pulls positrons in the opposite direction, acting against their guiding.

In the context of DLA driven by a high-intensity laser pulse ($\geq 10^{23}$ W/cm^2), the central electron beam density increases with the propagation distance. Ions can be injected and accelerated along the channel axis [55,62], thus reducing the positive radial electric field $|E_c|$ [56,57]. In addition, the electron beam loading is enhanced by a radiative trapping [55,56]. An excess of negative charge is thus progressively built up at the channel center, inducing a negative charge separation field $\mathbf{E}_{e-} = -|E_{e-}|\mathbf{r}$, which can overcome the positive, self-generated field $\mathbf{E}_c$ formed by the initial expulsion of the electrons $|E_{e-}| > |E_c|$. This superposition results in a radial channel electric field amplitude $|E_c| - |E_{e-}| < 0$ guiding positive charges on axis.

We demonstrate the existence of a region focusing on positrons using PIC simulations. In the upper panel of
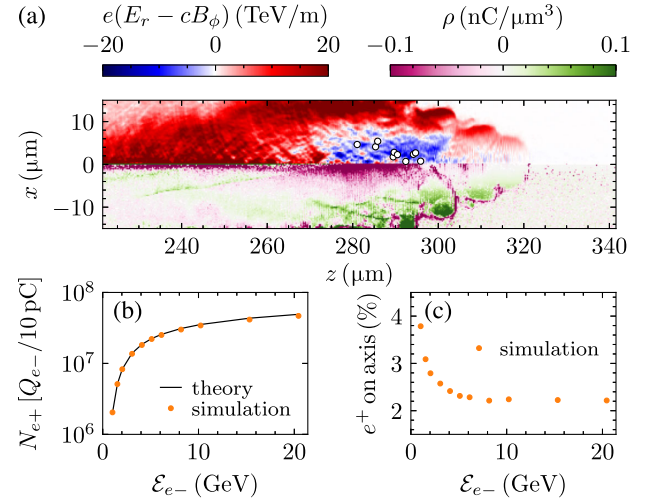

FIG. 2. Positron guiding and injection. (a) Electron beam loading after 280 μm of propagation. Upper panel: channel fields contribution to the transverse Lorentz force on the positrons ($m = 0$). Lower panel: net plasma charge density. (b) The number of generated positrons; (c) The fraction of positrons injected in the laser propagation direction as a function of the electron beam energy for a laser field amplitude 5×10^{23} W/cm^2 (circles). Panel (b) shows the number of positrons generated using an electron beam of 10 pC and can be directly scaled to different beams (e.g., $Q_{e-} = 100$ pC would give 10 times more positrons).

Fig. 2(a), we represent the transverse Lorentz force induced by the channel fields (mode 0) on positrons (white circles). After 280 μm of propagation, the force is negative in the blue region ($275 \leq z \leq 300$ μm and $r \leq 10$ μm). The lower panel of Fig. 2(a) displays the total charge density (including all plasma species) where we observe an excess of negative charges associated with electron beam loading ($\simeq 800$ nC). The spatial structure of this beam generates a region of space where positrons are stably guided over 100s of micrometers.

III. POSITRON CREATION AND DIRECT LASER ACCELERATION

Now that we established the feasibility of positron guiding, we focus the discussion on positron creation, injection, and acceleration. The number of positrons generated at the laser focus can be evaluated by adapting a semianalytical model [39,63,64] for our specific interaction geometry. In Ref. [39], the authors derive the probability of a single photon decay $P_{\pm}$ in a head-on collision with a plane wave with a temporal envelope. In the Supplementary Material [61], we generalize this model to an arbitrary angle of incidence. We further enriched this model to account for a focused pulse interacting with a photon beam, which has a Gaussian shape in the z direction (3 μm FWHM) and is uniform in the radial direction. Each photon in the beam experiences an effective peak field amplitude denoted a, which is smaller than the maximum pulse amplitude [63]. The photons can be binned according to the maximum field they interact with, which defines a new distribution dN/da. The total number of positrons is thus obtained by integrating the probability $P_{\pm}$ over the distribution dN/da. Assuming that the interacting photons have a Quantum synchrotron spectrum $dN_{\mathrm{IC}}/d\gamma_{\gamma}dt$ of a monoenergetic electron beam with energy $\mathcal{E}_{e-}$ [65], we get

$$N_{e+} = \int_{\gamma_{\gamma}} \int_{a} \left(\frac{dN_{\mathrm{IC}}}{d\gamma_{\gamma}dt} \times \frac{dN}{da} \times P_{\pm} \right) \Big/ \left(\frac{dN_{\mathrm{IC}}}{dt} \right) \quad (1)$$

where $P_{\pm}$ is our generalized theoretical decay probability for one gamma ray in a plane wave [61].

The semianalytical estimate in Eq. (1) provides the number of positrons that one could create within a plasma channel. The accuracy for different electron beam energies is confirmed via PIC simulations displayed in Fig. 2(b). The peak laser amplitude is 5×10^{23} W/cm². We considered electron beam energies $\mathcal{E}_{e-}$ between 1 and 20 GeV to cover the range available either from plasma or conventional sources. The theory is valid in the limit where most pairs are created as a result of the decay of initial photons (no secondary pairs are accounted for). As expected, Fig. 2(b) shows that the number of positrons is an increasing function of the electron beam energy. The number of pairs in the simulation is well approximated by Eq. (1), which can therefore be used to quickly identify

optimal incident electron beam energies for future experiments. Our modeling indicates that the number of positrons (created and deflected) linearly depends on the charge of electrons interacting with the laser focal volume. For instance, using a 100-pC laser-driven beam would generate 10 times more positrons than obtained in Fig. 2(b).

Following their creation, positrons have a momentum perpendicular to the laser propagation direction. Simulations show that only a fraction of these can be deflected toward the laser propagation direction and later accelerated, see Fig. 2(c). These PIC simulations account for secondary pair production. The efficiency of deflection is maximized (4%) for the lowest value of incident electron beam energy $\mathcal{E}_{e-} \sim 1$ GeV. Such beams produce on average lower energy positrons, which are more prone to be redirected in the laser propagation direction [43]. This trend is confirmed in the Supplementary Material [61], where we derived an estimate of the number of low-energy positrons created.

Once injected within the channel, positrons can be affected by the laser field and the nonlinear plasma response. Both laser and channel fields have longitudinal and transverse electric components (with respect to the laser axis), shown in Figs. 3(a) and 3(b). We note that due to electron beam loading, the transverse electric field generated in the channel has a negative sign in a large region, attracting positrons on axis (~ 10 TV/m). As it propagates, the laser pulse undergoes self-focusing [66]. Depending on
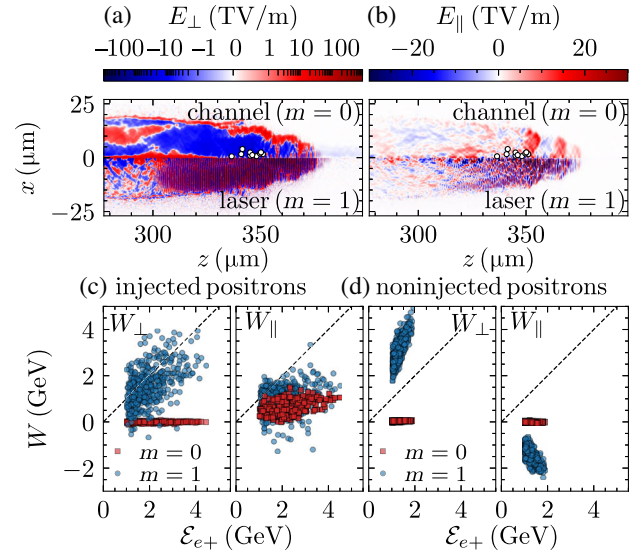

FIG. 3. Positron direct laser acceleration. (a) Transverse electric field (x direction). White circles represent a sample of injected positrons. Mode $m = 1$ is associated with the laser component, while $m = 0$ represents the channel field. (b) Longitudinal electric field (z direction). (c) Energy gain of injected positrons in transverse ($W_{\perp}$) and longitudinal directions ($W_{\parallel}$). (d) Energy gain of noninjected positrons. The energy gains W represent the accumulated work in the channel fields ($m = 0$, red squares) and the laser fields ($m = 1$, blue circles) after a propagation distance of 340 μm.

the background plasma density, the self-focusing dynamics can be affected by parametric plasma instabilities. In addition, our study is in the relativistic regime, where also radiation reaction effects can become important due to the high laser intensity. Even though the nonlinear interplay of all these effects is not possible to predict analytically, they are all naturally incorporated in the QED-PIC simulations, which we can use to model the laser pulse guiding. We observed that the laser field amplitude is still strong ($\gtrsim$200 TV/m) even after 340 μm of propagation due to relativistic self-focusing. Apart from strong transverse fields, both the longitudinal channel field (due to local charge separations) and the longitudinal laser field (due to relativistic self-focusing) are significant.

The total contribution of each field component for the positron energy gain (W) is studied in Fig. 3(c). We show a scatter plot for 500 injected positrons, where the x axis denotes their final energy ($\mathcal{E}_{e+}$) and the y axis shows the total work of different E field components. We consider positrons injected if they remain inside the plasma channel after 420 μm of laser propagation. The energy gains W are decomposed in the perpendicular/longitudinal direction $W_{\perp/\parallel} = \int \mathbf{v} \cdot \mathbf{E}_{\perp/\parallel} dt$. They are further split between the contribution of the channel fields ($m = 0$) and the laser ($m = 1$). This analysis is repeated in Fig. 3(d) for 500 noninjected positrons. The first result is that injected positrons in Fig. 3(c) achieve energies of 4 GeV, whereas the noninjected positrons in Fig. 3(d) are limited below 2 GeV. By definition, noninjected positrons are not trapped in the guiding structure in Fig. 2(a). They experience a partial acceleration in the laser pulse, but they cannot be collected on a detector after the plasma channel because they leave the interaction region sideways. Overall, the direct contribution of transverse channel fields for acceleration is small (though it is responsible for guiding). The parallel component of the laser plays a role for all positrons, but the work performed is purely negative for positrons deflected outside the channel. For injected positrons in Fig. 3(c), we observe that the energy gain from the transverse laser field component $W_\perp$ can be as high as 4 GeV, while the longitudinal energy gains both from the laser and the channel fields are limited below 1.5 GeV. This indicates that DLA prevails over other possible mechanisms (e.g., laser or beam-driven wakefield acceleration). We also observed the forking structure characterizing DLA [67,68]. The two beam sections are ejected at an angle ±10° with a divergence of 50 mrad.

The charge content and energy spectrum of the positron beam are summarized in Fig. 4. The number of positrons is shown as a function of the laser propagation distance within the channel. Most positrons are created in the first ∼100 μm of propagation. From 100 to 220 μm, the electrons are injected, forming a tenuous beam of increasing density. The channel fields are still defocusing positrons during this time, thus explaining the large decrease in
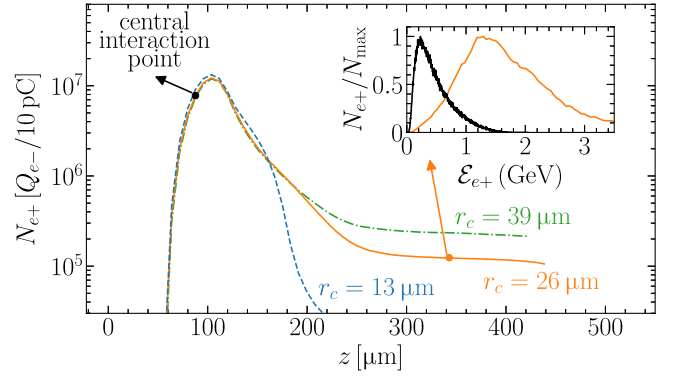

FIG. 4. The number of injected positrons as a function of the laser propagation distance for different channel sizes. The black circle marks the central interaction point of the laser pulse with the photon beam. Inset: Positron energy spectrum for $r_c = 26$ μm at creation time (black). The total charge is 1.3 pC and $N_{\max} = 6$ pC/GeV. Positron spectrum at $z = 340$ μm. The total charge is 17 fC and $N_{\max} = 12$ fC/GeV. The normalization facilitates the scaling of the result to a higher electron beam charge.

N_{e+}. From 220 to 420 μm, the number of positrons is constant since the electron beam loading is large enough to create the field structure guiding positrons. Beyond 420 μm, the guiding structure cannot be maintained as the laser gets depleted ($\gtrsim$30% energy loss). The acceleration distance in experiments should therefore be limited below 400 μm to avoid reduction of the injected charge.

The plasma channel size influences the injection process. For the channel with a small radius (13 μm), ions are loaded at the channel center on top of the positrons. This motion reduces the negative charge separation field and defocuses positrons. However, for larger channel widths, the positrons can be guided efficiently as the ions lag behind the positrons. Please note that the plasma is assumed to be a fully ionized nitrogen gas, with a charge-to-mass ratio of 1/2. If one were to use a lighter species (e.g., protons, with a charge-to-mass ratio of 1), the time scale for acceleration would be smaller, and a wider channel would be required to form a similar guiding structure. For the case of a nitrogen plasma with a radius $r_c = 26$ μm, the total charge of the positron beam after 340 μm of propagation is 17 fC. Its energy spectrum shown as an inset in Fig. 4 evidences positron acceleration from 0.22 GeV at creation time, up to 1.3 GeV after 340 μm of laser propagation. Higher energies ∼5–10 GeV could be reached in future work, based on scaling laws for electron DLA with multi-PW lasers [51].

IV. DISCUSSION AND CONCLUSION

We now compare our findings with other schemes one can find in the literature. Postacceleration setups provide a higher charge and beam quality [6–21], but they are not compact as they require a kilometer-long accelerator. The strength of our method is that positrons are both created and

accelerated to a GeV level in a single, sub-millimeter stage. Other setups that consider multi-PW lasers, either focus only on pair creation without acceleration [37–40] or use 2D geometry which does not allow for reliable quantitative predictions for the number and energy of the accelerated positrons [41–45]. For the first time, our quasi-3D approach allows obtaining quantitative estimates for a compact single-stage positron creation and acceleration scheme.

In conclusion, our work opens the possibility for direct laser acceleration of positrons in a plasma. We demonstrate that it is possible to create, inject, and accelerate positrons in a single-stage experiment by laser-electron scattering at 90°. We develop an analytical model to estimate the number of created positrons in this geometry and determine with simulations that about 4% of these particles are injected and accelerated. The essential feature for positron guiding is the self-injected electron beam in the channel center ($\sim$800 nC). It enables positron acceleration to multi-GeV energies in less than a millimeter of laser propagation.

The presented positron acceleration scheme can be realized with the next generation of laser facilities that will reach 75–200 PW [27–31]. A minimum power of $\sim$80 PW, is required to drive a copious pair production and an efficient positron injection. Increasing the power further would enhance the number of injected positrons. The incident electron beam considered (10 pC at 2 GeV) can already be produced experimentally [69–72]. For the preformed plasma, we suggest to use a commercially available, dense ($10^{21}/\text{cm}^3$), and short (400 μm) plasma jet [73] and to control the channel radius as in Ref. [74]. The femtosecond and micrometer synchronization was already achieved [33] and could be less restrictive using larger-scale, laser-driven DLA electron beams [67,68,75–79]. Our setup generates a broadband beam of GeV-class electrons, positrons, and gamma-rays, which opens a new avenue of opportunities for QED cascade seeding or the study of the propagation of a fireball jet within a plasma in a laboratory setting.

[1] T. Tajima and J. M. Dawson, Phys. Rev. Lett. 43, 267 (1979).

[2] J. S. T. Ng, P. Chen, H. Baldis, P. Bolton, D. Cline, W. Craddock, C. Crawford, F. J. Decker, C. Field, Y. Fukui, V. Kumar, R. Iverson, F. King, R. E. Kirby, K. Nakajima, R. Noble, A. Ogata, P. Raimondi, D. Walz, and A. W. Weidemann, Phys. Rev. Lett. 87, 244801 (2001).

[3] M. J. Hogan, C. E. Clayton, C. Huang, P. Muggli, S. Wang, B. E. Blue, D. Walz, K. A. Marsh, C. L. O'Connell, S. Lee, R. Iverson, F.-J. Decker, P. Raimondi, W. B. Mori, T. C. Katsouleas, C. Joshi, and R. H. Siemann, Phys. Rev. Lett. 90, 205002 (2003).

[4] B. E. Blue, C. E. Clayton, C. L. O'Connell, F.-J. Decker, M. J. Hogan, C. Huang, R. Iverson, C. Joshi, T. C. Katsouleas, W. Lu, K. A. Marsh, W. B. Mori, P. Muggli, R. Siemann, and D. Walz, Phys. Rev. Lett. 90, 214801 (2003).

[5] P. Muggli, B. E. Blue, C. E. Clayton, F. J. Decker, M. J. Hogan, C. Huang, C. Joshi, T. C. Katsouleas, W. Lu, W. B. Mori, C. L. O'Connell, R. H. Siemann, D. Walz, and M. Zhou, Phys. Rev. Lett. 101, 055001 (2008).

[6] S. Corde et al., Nature (London) 524, 442 (2015).

[7] S. Gessner et al., Nat. Commun. 7, 11785 (2016).

[8] A. Doche et al., Sci. Rep. 7, 14180 (2017).

[9] C. A. Lindstrøm et al., Phys. Rev. Lett. 120, 124802 (2018).

[10] N. Jain, T. M. Antonsen, and J. P. Palastro, Phys. Rev. Lett. 115, 195001 (2015).

[11] J. Vieira and J. T. Mendonça, Phys. Rev. Lett. 112, 215001 (2014).

[12] Y. Li, G. Xia, K. V. Lotov, A. P. Sosedkin, and Y. Zhao, Plasma Phys. Controlled Fusion 61, 025012 (2019).

[13] C. S. Hue, G. J. Cao, I. A. Andriyash, A. Knetsch, M. J. Hogan, E. Adli, S. Gessner, and S. Corde, Phys. Rev. Res. 3, 043063 (2021).

[14] T. C. Chiou, T. Katsouleas, C. Decker, W. B. Mori, J. S. Wurtele, G. Shvets, and J. J. Su, Phys. Plasmas 2, 310 (1995).

[15] C. B. Schroeder, D. H. Whittum, and J. S. Wurtele, Phys. Rev. Lett. 82, 1177 (1999).

[16] X. Wang, R. Ischebeck, P. Muggli, T. Katsouleas, C. Joshi, W. B. Mori, and M. J. Hogan, Phys. Rev. Lett. 101, 124801 (2008).

[17] W. D. Kimura, H. M. Milchberg, P. Muggli, X. Li, and W. B. Mori, Phys. Rev. ST Accel. Beams 14, 041301 (2011).

[18] L. Yi, B. Shen, L. Ji, K. Lotov, A. Sosedkin, XiaomeiZhang, W. Wang, J. Xu, Y. Shi, L. Zhang, and Z. Xu, Sci. Rep. 4, 4171 (2014).

[19] S. Diederichs, T. J. Mehrling, C. Benedetti, C. B. Schroeder, A. Knetsch, E. Esarey, and J. Osterhoff, Phys. Rev. Accel. Beams 22, 081301 (2019).

[20] T. Silva, L. D. Amorim, M. C. Downer, M. J. Hogan, V. Yakimenko, R. Zgadzaj, and J. Vieira, Phys. Rev. Lett. 127, 104801 (2021).

[21] L. Reichwein, A. Pukhov, A. Golovanov, and I. Y. Kostyukov, Phys. Rev. E 105, 055207 (2022).

[22] T. Heinzl and A. Ilderton, Eur. Phys. J. D 55, 359 (2009).

[23] D. N. Papadopoulos, J. P. Zou, C. L. Blanc, L. Ranc, F. Druon, L. Martin, A. Fréneaux, A. Beluze, N. Lebas, M. Chabanis, C. Bonnin, J. B. Accary, B. L. Garrec, F. Mathieu, and P. Audebert, in Proceedings of Conference

on Lasers and Electro-Optics (Optical Society of America, United States, 2019), p. STu3E.4, 10.1364/CLEO_SI.2019.STu3E.4.

[24] J. W. Yoon, C. Jeon, J. Shin, S. K. Lee, H. W. Lee, I. W. Choi, H. T. Kim, J. H. Sung, and C. H. Nam, Opt. Express **27**, 20412 (2019).

[25] A. Shaykin, I. Kostyukov, A. Sergeev, and E. Khazanov, Rev. Laser Eng. **42**, 141 (2014).

[26] C. Radier, O. Chalus, M. Charbonneau, S. Thambirajah, G. Deschamps, S. David, J. Barbe, E. Etter, G. Matras, S. Ricaud *et al.*, High Power Laser Sci. Eng. **10**, e21 (2022).

[27] J. Bromage, S.-W. Bahk, I. A. Begishev, C. Dorrer, M. J. Guardalben, B. N. Hoffman, J. Oliver, R. G. Roides, E. M. Schiesser, M. J. Shoup III *et al.*, High Power Laser Sci. Eng. **7**, e4 (2019).

[28] G. Mourou, G. Korn, W. Sandner, and J. Collier, THOSS Media GmbH (2011).

[29] B. Shao, Y. Li, Y. Peng, P. Wang, J. Qian, Y. Leng, and R. Li, Opt. Lett. **45**, 2215 (2020).

[30] A. V. Bashinov, A. A. Gonoskov, A. V. Kim, G. Mourou, and A. M. Sergeev, Eur. Phys. J. Spec. Top. **223**, 1105 (2014).

[31] G. Mourou, N. Fisch, V. Malkin, Z. Toroker, E. Khazanov, A. Sergeev, T. Tajima, and B. Le Garrec, Opt. Commun. **285**, 720 (2012).

[32] D. L. Burke, R. C. Field, G. Horton-Smith, J. E. Spencer, D. Walz, S. C. Berridge, W. M. Bugg, K. Shmakov, A. W. Weidemann, C. Bula, K. T. McDonald, E. J. Prebys, C. Bamber, S. J. Boege, T. Koffas, T. Kotseroglou, A. C. Melissinos, D. D. Meyerhofer, D. A. Reis, and W. Ragg, Phys. Rev. Lett. **79**, 1626 (1997).

[33] K. Poder *et al.*, Phys. Rev. X **8**, 031004 (2018).

[34] N. Neitz and A. Di Piazza, Phys. Rev. Lett. **111**, 054802 (2013).

[35] T. G. Blackburn, C. P. Ridgers, J. G. Kirk, and A. R. Bell, Phys. Rev. Lett. **112**, 015001 (2014).

[36] F. Niel, C. Riconda, F. Amiranoff, R. Duclous, and M. Grech, Phys. Rev. E **97**, 043209 (2018).

[37] I. V. Sokolov, N. M. Naumova, J. A. Nees, and G. A. Mourou, Phys. Rev. Lett. **105**, 195005 (2010).

[38] M. Lobet, X. Davoine, E. d'Humières, and L. Gremillet, Phys. Rev. Accel. Beams **20**, 043401 (2017).

[39] T. G. Blackburn, A. Ilderton, C. D. Murphy, and M. Marklund, Phys. Rev. A **96**, 022128 (2017).

[40] M. J. V. Streeter, C. Colgan, N. Cavanagh, E. Los, A. F. Antoine, T. Audet, M. D. Balcazar, L. Calvin, J. Carderelli, H. Ahmed, B. Kettle, Y. Ma, S. P. D. Mangles, Z. Najmudin, P. P. Rajeev, D. R. Symes, A. G. R. Thomas, and G. Sarri, arXiv:2205.13850.

[41] H. Chen *et al.*, Phys. Rev. Lett. **105**, 015003 (2010).

[42] Y. Yan, Y. Wu, J. Chen, M. Yu, K. Dong, and Y. Gu, Plasma Phys. Controlled Fusion **59**, 045015 (2017).

[43] M. Vranic, O. Klimo, G. Korn, and S. Weber, Sci. Rep. **8**, 4702 (2018).

[44] Z. Xu, L. Yi, B. Shen, J. Xu, L. Ji, T. Xu, L. Zhang, S. Li, and Z. Xu, Commun. Phys. **3**, 191 (2020).

[45] Y. He, T. G. Blackburn, T. Toncian, and A. V. Arefiev, Commun. Phys. **4**, 139 (2021).

[46] A. Pukhov, Z.-M. Sheng, and J. Meyer-ter Vehn, Phys. Plasmas **6**, 2847 (1999).

[47] A. V. Arefiev, B. N. Breizman, M. Schollmeier, and V. N. Khudik, Phys. Rev. Lett. **108**, 145004 (2012).

[48] A. V. Arefiev, V. N. Khudik, A. P. L. Robinson, G. Shvets, L. Willingale, and M. Schollmeier, Phys. Plasmas **23**, 056704 (2016).

[49] V. Khudik, A. Arefiev, X. Zhang, and G. Shvets, Phys. Plasmas **23**, 103108 (2016).

[50] Z. Gong, F. Mackenroth, T. Wang, X. Q. Yan, T. Toncian, and A. V. Arefiev, Phys. Rev. E **102**, 013206 (2020).

[51] M. Jirka, M. Vranic, T. Grismayer, and L. O. Silva, New J. Phys. **22**, 083058 (2020).

[52] T. Wang, D. Blackman, K. Chin, and A. Arefiev, Phys. Rev. E **104**, 045206 (2021).

[53] F.-Y. Li, P. K. Singh, S. Palaniyappan, and C.-K. Huang, Phys. Rev. Accel. Beams **24**, 041301 (2021).

[54] I.-L. Yeh, K. Tangtartharakul, H. G. Rinderknecht, L. Willingale, and A. Arefiev, New J. Phys. **23**, 095010 (2021).

[55] L. L. Ji, A. Pukhov, I. Y. Kostyukov, B. F. Shen, and K. Akli, Phys. Rev. Lett. **112**, 145003 (2014).

[56] M. Vranic, R. A. Fonseca, and L. O. Silva, Plasma Phys. Controlled Fusion **60**, 034002 (2018).

[57] T. Wang, Z. Gong, K. Chin, and A. Arefiev, Plasma Phys. Controlled Fusion **61**, 084004 (2019).

[58] R. A. Fonseca, L. O. Silva, F. S. Tsung, V. K. Decyk, W. Lu, C. Ren, W. B. Mori, S. Deng, S. Lee, T. Katsouleas, and J. C. Adam, in *Computational Science—ICCS 2002*, edited by P. M. A. Sloot, A. G. Hoekstra, C. J. K. Tan, and J. J. Dongarra (Springer, Berlin, Heidelberg, 2002), pp. 342–351, 10.1007/3-540-47789-6_36.

[59] A. Lifschitz, X. Davoine, E. Lefebvre, J. Faure, C. Rechatin, and V. Malka, J. Comput. Phys. **228**, 1803 (2009).

[60] A. Davidson, A. Tableman, W. An, F. Tsung, W. Lu, J. Vieira, R. Fonseca, L. Silva, and W. Mori, J. Comput. Phys. **281**, 1063 (2015).

[61] See Supplemental Material at http://link.aps.org/supplemental/10.1103/PhysRevAccelBeams.26.011301 for the derivation of the number of positrons, the fraction deflected and simulation parameters.

[62] E. G. Gelfer, A. M. Fedotov, and S. Weber, New J. Phys. **23**, 095002 (2021).

[63] Ó. Amaro and M. Vranic, New J. Phys. **23**, 115001 (2021).

[64] A. Mercuri-Baron, M. Grech, F. Niel, A. Grassi, M. Lobet, A. D. Piazza, and C. Riconda, New J. Phys. **23**, 085006 (2021).

[65] T. Erber, Rev. Mod. Phys. **38**, 626 (1966).

[66] G.-Z. Sun, E. Ott, Y. C. Lee, and P. Guzdar, Phys. Fluids **30**, 526 (1987).

[67] A. E. Hussein, A. V. Arefiev, T. Batson, H. Chen, R. S. Craxton, A. S. Davies, D. H. Froula, Z. Gong, D. Haberberger, Y. Ma, P. M. Nilson, W. Theobald, T. Wang, K. Weichman, G. J. Williams, and L. Willingale, New J. Phys. **23**, 023031 (2021).

[68] J. L. Shaw, N. Lemos, K. A. Marsh, D. H. Froula, and C. Joshi, Plasma Phys. Controlled Fusion **60**, 044012 (2018).

[69] A. J. Gonsalves *et al.*, Phys. Rev. Lett. **122**, 084801 (2019).

[70] X. Wang *et al.*, Nat. Commun. **4**, 1988 (2013).

[71] H. T. Kim, K. H. Pae, H. J. Cha, I. J. Kim, T. J. Yu, J. H. Sung, S. K. Lee, T. M. Jeong, and J. Lee, Phys. Rev. Lett. **111**, 165002 (2013).

[72] H. T. Kim, V. B. Pathak, K. Hong Pae, A. Lifschitz, F. Sylla, J. H. Shin, C. Hojbota, S. K. Lee, J. H. Sung, H. W. Lee, E. Guillaume, C. Thaury, K. Nakajima, J. Vieira, L. O. Silva, V. Malka, and C. H. Nam, Sci. Rep. **7,** 10203 (2017).

[73] F. Sylla, M. Veltcheva, S. Kahaly, A. Flacco, and V. Malka, Rev. Sci. Instrum. **83,** 033507 (2012).

[74] C. V. Pieronek, A. J. Gonsalves, C. Benedetti, S. S. Bulanov, J. van Tilborg, J. H. Bin, K. K. Swanson, J. Daniels, G. A. Bagdasarov, N. A. Bobrova, V. A. Gasilov, G. Korn, P. V. Sasorov, C. G. R. Geddes, C. B. Schroeder, W. P. Leemans, and E. Esarey, Phys. Plasmas **27,** 093101 (2020).

[75] O. N. Rosmej, X. F. Shen, A. Pukhov, L. Antonelli, F. Barbato, M. Gyrdymov, M. M. Günther, S. Zähter, V. S. Popov, N. G. Borisenko, and N. E. Andreev, Matter Radiat. Extremes **6,** 048401 (2021).

[76] M. M. Günther, O. N. Rosmej, P. Tavana, M. Gyrdymov, A. Skobliakov, A. Kantsyrev, S. Zähter, N. G. Borisenko, A. Pukhov, and N. E. Andreev, Nat. Commun. **13,** 170 (2022).

[77] C. Gahn, G. D. Tsakiris, A. Pukhov, J. Meyer-ter Vehn, G. Pretzler, P. Thirolf, D. Habs, and K. J. Witte, Phys. Rev. Lett. **83,** 4772 (1999).

[78] S. Jiang, L. L. Ji, H. Audesirk, K. M. George, J. Snyder, A. Krygier, P. Poole, C. Willis, R. Daskalova, E. Chowdhury, N. S. Lewis, D. W. Schumacher, A. Pukhov, R. R. Freeman, and K. U. Akli, Phys. Rev. Lett. **116,** 085002 (2016).

[79] L. Willingale, A. V. Arefiev, G. J. Williams, H. Chen, F. Dollar, A. U. Hazi, A. Maksimchuk, M. J.-E. Manuel, E. Marley, W. Nazarov, T. Z. Zhao, and C. Zulick, New J. Phys. **20,** 093024 (2018).